ISSN1027-5495. Functional Materials, 31, No.4 (2024), p. 487-494
doi:http://dx.doi.org/10.15407/fm31.04.487

Structure refinement, ferroelectric domains and mechanical properties of Czochralski-grown $Ca_9La(VO_4)_7$ and $Ca_{10}Li(VO_4)_7$ single crystals

V.A. Bedarev [1], M.B. Kosmyna [2], P.V. Mateychenko [2], D.N. Merenkov [1], W. Paszkowicz [3], S.N. Poperezhai [1], A. Fitch [4], P. Romanowski [3], A.N. Shekhovtsov [2]

[1] B. Verkin Institute for Low Temperature Physics and Engineering, NAS of Ukraine, Nauky Ave. 47, 61103, Kharkov, Ukraine
[2] Institute for Single Crystals, NAS of Ukraine, Nauky Ave. 60, 61072, Kharkov, Ukraine·
[3] Institute of Physics, Polish Academy of Sciences, Aleja Lotnikow 32/46, PL-02668 Warsaw, Poland
[4] ESRF, CS40220, 38043 Grenoble Cedex 9, France

Received July,5, 2005

Physical properties of whitlockite-type $Ca_3(VO_4)_2$ orthovanadate can be modified by incorporation of isovalent or aliovalent cation substituents. In this paper, the features of the crystal structure of $Ca_9La(VO_4)_7$ and $Ca_{10}Li(VO_4)_7$ whitlockite-type crystals grown by the Czochralski method with substitution by aliovalent La or Li ions are studied. Refinement of the structure using the Rietveld approach allowed us to determine the unit cell parameters and site occupancy. According to the data of polarization-optical studies, the formation of a strip-like ferroelectric domain structure with spontaneous polarization parallel to the third-order axis was established in the $Ca_9La(VO_4)_7$ single crystal. It has been established that $Ca_{10}Li(VO_4)_7$ is an antiferroelectric at room temperature. The correlations between Vickers hardness and fracture toughness values and the degree of crystal perfection are discussed.

Keywords: powder diffraction, orthovanadate, whitlockite, ferroelectric domain, crystal structure.

Уточнення кристалічної структури, сегнетоелектричні домени та механічні властивості монокристалів $Ca_9La(VO_4)_7$ і $Ca_{10}Li(VO_4)_7$ вирощених методом Чохральського. *В.А. Бедарєв, М.Б. Космина, П.В. Матейченко, Д.М. Меренков, В. Пашкович, С.М. Попережай, А. Фіч, П. Романовський, О.М. Шеховцов*

Фізичні властивості ортованадату кальцію $Ca_3(VO_4)_2$, який належить до структурного типу «вітлокіт» можуть бути модифіковані шляхом изо- або гетеровалентного заміщення кальцію. В роботі досліджені властивості кристалічної структури кристалів $Ca_9La(VO_4)_7$ та $Ca_{10}Li(VO_4)_7$ вирощених методом Чохральського, які належать до структурного типу «вітлокіт» та утворені шляхом гетеровалентного заміщення атомами La та Li, відповідно. За результатами уточнення структури, виконаним методом Рітвельда, отримані дані про параметри елементарної комірки та заповненість кристалографічних позицій. За даними поляризаційно-оптичних досліджень встановлено, що в монокристалі $Ca_9La(VO_4)_7$ формується «стрічкова» сегнетоелектрична доменна структура зі спонтанною поляризацією, паралельною осі третього порядку. Виявлено, що $Ca_{10}Li(VO_4)_7$ є антисегнетоелектриком при кімнатній температурі. Була обговорена кореляція мікротвердості та в'язкості руйнування зі ступенем структурної досконалості кристалів.

1. Introduction

Tricalcium vanadate $Ca_3(VO_4)_2$ (TCV) and ß-tricalcium phosphate (ß-$Ca_3(VO_4)_2$, ß-TCP) crystallize in the whitlockite type structure ß-$Ca_3(PO_4)_2$. The whitlockite-type structure allows for designing a variety of ternary and multinary orthovanadates/orthophosphates with modified composition and specified properties. Namely, the whitlockite-type structure easily allows fractional substitution of Ca ions by isovalent or aliovalent ions. Typically, such modified oxides crystallize in the same noncentrosymmetric space group, $R3c$; some of them have been reported to adopt the centrosymmetric $R\,\bar{3}c$ space group with a unit cell of the same size. Whitlockite-related materials form an extended family of compounds. Among them are those that are substituted with aliovalent (monovalent or trivalent) dopants fractionally occupying Ca sites. In particular, these are binary orthovanadates or phosfates of common formula $Ca_9RE(AO_4)_7$ (A = P or V, RE = lanthanide or yttrium); other trivalent elements can be substituents, as well. Related compounds have been reported for monovalent substituents, with formula $Ca_{10}M(AO_4)_7$ (M = alkali element or Cu, Ag).

The structure of $Ca_3(AO_4)_2$ consists of isolated vertex-sharing $(AO_4)^{3-}$ tetrahedra forming a three-dimensional skeleton. Calcium cations occupy five non-equivalent crystallographic sites. The unit cell includes structural vacancies at the M4 sites (in $Ca_3(AO_4)_2$, this site is half occupied by Ca ions). Binary orthovanadates and orthophosphates are formed by fractional introduction of various iso- or aliovalent substituents into calcium sites.

In the $Ca_{10}M^+(AO_4)_7$ (M = Li, Na, K, A = P, V) unit cell, the M atoms fully occupy the M4 site. When forming $Ca_{10}M(AO_4)_7$ compounds, substitution of calcium occurs according to the scheme:

$$0.5(Ca^{2+} + \square) = M^+, \quad (1)$$

where □ represents a vacancy. The substitution leads to the full occupation of M4 site by an alkali element. Unit cells of $Ca_{10}M(AO_4)_7$ compounds do not contain structural vacancies.

In the unit cell of $Ca_9RE^{3+}(AO_4)_7$ (RE = lanthanides and Y, A = P, V), the RE atoms simultaneously occupy several (from among M1, M2, M3, M5) sites with fractional occupancy depending on the selected RE atom. The formation of $Ca_9RE(VO_4)_7$ compounds occurs when calcium is replaced by the RE element according to the scheme:

$$1.5Ca^{2+} = RE^{3+} + 0.5\nu \quad (2)$$

Vacancies in $Ca_9RE(VO_4)_7$ are located at the Ca4 site. In this structure, RE cations are distributed in several sites [1-5]. The distribution of RE ions in these sites depends on the selected RE atom. In the above formulas, the M and RE content can be fractional, i.e. less than indicated in the formulas above.

Various vanadates with whitlockite-type structure exhibit interesting optical properties [6, 7]. $Ca_9RE(VO_4)_7$ and other orthovanadates with whitlockite-type structure (as well s orthophosphates) are being considered for applications in optoelectronics, such as in white- LEDs and as materials for tunable lasers [8]. Substituted non-centrosymmetric TCVs or ß-TCPs are expected to be efficient second harmonic generation materials. Namely, the efficient second harmonic generation has been demonstrated for a number of vanadate single crystals [7, 9-11] and polycrystals [12, 13]. Moreover, efficient laser operation for Nd-doped $Ca_9La(VO_4)_7$ and $Ca_{10}Li(VO_4)_7$ single crystals has been shown in [14,15] respectively.

$Ca_9La(VO_4)_7$ and $Ca_{10}Li(VO_4)_7$ belong to a series of whitlockite-related materials crystallizing in the space group $R3c$ [1]. The synthesis of polycrystalline $Ca_9La(VO_4)_7$ (LaTCV) has previously been performed by various methods such as solid state synthesis [1, 16, 17] and sol-gel technique [18]. The Czochralski method has been used to grow single crystals of this compound [19, 20]. Data on the $Ca_9La(VO_4)_7$ crystal structure are available in [1].

For doped $Ca_9La(VO_4)_7$ and $Ca_{10}Li(VO_4)_7$, the optical characteristics has been studied only recently. The spectral properties of LaTCV doped with various rare-earth elements have been reported to make these crystals suitable for white LEDs [21, 22]; tunable white light emission are considered in [17]. Efficient phosphors based on $B_9Ln(VO_4)_7$ (B = Ca, Sr, Ba, Ln = La or Gd) compounds have been described in [16]. When excited in the range of 300-400 nm, emission covering the spectral range of 400-650 nm was observed.

The nature of the intensity parameter Ω_2 and the associated line strength, S, of the $^4I_{9/2} \rightarrow {}^4G_{5/2}$ hypersensitive transition of Nd^{3+} has been studied in [23] for Nd-doped binary orthovanadates including $Ca_9La(VO_4)_7$ and

$Ca_{10}Li(VO_4)_7$. It has been shown, that the parameter Ω_2 and the line strength S weakly depend on the covalence of the bonds of neodymium and ligand ions, and are mainly determined by the symmetry of the neodymium local environment in the crystal lattice.

One of the features of whitlockite-type crystals is the presence of a ferroelectric phase transition in the range of 1000-1300 K in some of the known systems, for example, in $Ca_9RE(VO_4)_7$ [24], $Ca_9In(PO_4)_7$ [25], and $Ca_9Fe(PO_4)_7$ [26]. The ferroelectric nature of the phase transition in $Ca_9Y(VO_4)_7$ single crystal grown by the Czochralski method is confirmed by results of dielectric measurements [27, 28]. Moreover, it has been shown, that fractional substitution of the vanadate group in the $Ca_9Y(VO_4)_7$ single crystal by the phosphate group can dramatically affect the ferroelectric properties.

It is noteworthy that for a single crystal of the solid solution $Ca_9Y(VO_4)_3(PO_4)_4$, a centrosymmetric crystal structure (space group $R\ \bar{3}c$) has been determined at room temperature, differing only in details of atomic arrangement in the unit cell of the whitlockite type; however, the ferroelectric phase transition was not observed [27]. The ferroelectric transition was found for a polycrystalline sample of $Ca_9La(VO_4)_7$ at temperature T_c = 1173 K [24] based on an analysis of the temperature dependences of conductivity and dielectric permittivity. This material is reported as suitable for tunable lasing [29]. A similar "order-disorder" phase transition was not observed for the $Ca_{10}Li(VO_4)_7$ polycrystal. $Ca_{10}La(VO_4)_7$ has also been considered as a potential medium for 2 μm lasers [30].

Both $Ca_9La(VO_4)_7$ and $Ca_{10}Li(VO_4)_7$ crystals are electrically ordered at room temperature. Therefore, we can assume that "order-disorder" phase transitions can occur in the $Ca_{10}Li(VO_4)_7$ crystal, as well as in other vanadates with a polar whitlockite-type crystal structure. The phase transition of ferroelectric ordering is accompanied by the emergence of spontaneous electrical polarization in a crystal and the emergence of a domain structure. $Ca_9La(VO_4)_7$ and $Ca_{10}Li(VO_4)_7$ crystals are quite transparent in the visible light range. Thus, the electric domain structure in these crystals can be investigated using the polarization-optical method.

The aim of the present study was to characterize the domains which can be formed in $Ca_9La(VO_4)_7$ and $Ca_{10}Li(VO_4)_7$ crystals, by means of polarized optical method. The correlations between mechanical properties, chemical compositions, and structure were analyzed.

2. Experimental

A solid state synthesis was carried out to produce $Ca_9La(VO_4)_7$ and $Ca_{10}Li(VO_4)_7$ according to the following reactions:

$$18CaCO_3 + 7V_2O_5 + R_2O_3 \rightarrow \rightarrow 2Ca_9R(VO_4)_7 + 18CO_2\uparrow \quad (3)$$

$$20CaCO_3 + 7V_2O_5 + Li_2CO_3 \rightarrow \rightarrow 2Ca_{10}Li(VO_4)_7 + 21CO_2\uparrow \quad (4)$$

where R = La or La+Yb. The initial components were in the form of dried $CaCO_3$ (99.99%), Li_2CO_3 (99.99), R_2O_3 (99.99) (R = La, or La+Yb). The concentration of Yb in the charge was 15 at. %. The crystal growth was carried out along the [001] crystallographic axis by the Czochralski method [31] in argon atmosphere from crucibles of 60 mm diameter and 70 mm length. "Kristall 3M" apparatus equipped with an inductive heating and an automated diameter control system of growing crystal was used. The pulling rate varied within 1 – 3 mm/h and the rotational speed was varied in the range of 5 – 25 rpm. When using both active and passive heaters, the radial temperature gradient on the melt surface did not exceed 0.5 K/mm; the axial temperature gradient on the melt–argon interface was 75 K/cm. The crystal–melt interface was convex. To minimize thermoelastic stresses after the detachment of crystals, the ingot was kept above the melt for 2 h and cooled to room temperature for 24 h. For details of crystal growth, see [19, 15].

The crystal structure of $Ca_9R(VO_4)_7$ (R – La, La+Yb), was refined using the Rietveld method for powder diffraction data collected with both the laboratory and synchrotron equipment. For powder X-ray diffraction (XRD) experiments, the polycrystalline material was prepared from single crystals by crushing the crystals in an agate mortar. The laboratory Bragg-Brentano XRD measurements were carried out in Cu$K\alpha_1$ radiation using a Philips X'Pert PRO Alpha1 diffractometer [32] equipped with a Ge(111) primary-beam Johansson monochromator and a 127-element X'Celerator strip detector (constructed according to the idea first presented in [33]). The principles of the high-resolution powder diffraction method in a version using reflection geometry were developed in [34]. High-resolution synchrotron radiation (HRS) powder diffraction data were collected at the ID22 facility (Grenoble, France), using a parallel-beam capillary-transmission geometry (for description of similar settings, see

refs. [35, 36]; this setting provides the resolution of 0.0015° defined as the peak width for a $Na_2Ca_3Al_2F_{14}$ standard at 2θ = 7° [36]). The detection system was based on a bank of nine detectors preceded by Si(111) analyzer crystals. The data collection time was 1.25 h. The use of a highly collimated incident beam of ultra-short wavelength X-rays in combination with a crystal analyzer system provides high angular resolution and reduced background. Fast spinning of the capillary resulted in improved powder averaging. The structure was refined by the Rietveld method using the FullProf v.5.30 program [37].

To investigate the degree of perfection of the single crystals, high-resolution Philips MRD diffractometer equipped with a standard laboratory source of $Cu_{K\alpha 1}$ radiation (λ=1.54060 Å), an X-ray mirror and four bounce monochromator was used.

The elemental composition of single crystals was analyzed using a scanning electron microscope JEOL JSM-6390 equipped with an energy dispersive X-ray analyzer. An accuracy of measurements was ±5%.

A polarizing microscope equipped with a digital OMAX tool was used to study the domain structure at room temperature. The oriented samples were prepared in the form of plates with a thickness of 100 – 150 um. For minimization of mechanical stress induced by mechanical polishing, the samples were annealed at 550 – 600°C for 12 hours. The studies were carried out using linearly polarized white light passing along the third-order crystallographic axis, which coincides with the optical axis of $Ca_9La(VO_4)_7$ and $Ca_{10}Li(VO_4)_7$ crystals.

The hardness H_v of $Ca_9La(VO_4)_7$ and $Ca_{10}Li(VO_4)_7$ single crystals was determined by the indentation method using a Vickers diamond pyramid (PMT-3, load 50 g). The fracture toughness K_{1c} was determined according to [38]. Samples for the investigation were cut from the central cylindrical part of crystals.

3. Results and Discussion

$Ca_9La(VO_4)_7$ and $Ca_{10}Li(VO_4)_7$ single crystals were successfully grown by Czochralski method under the described conditions. The crystals had a diameter of 15-20 mm and a length of 60- 70 mm. Both samples were transparent and free of gas bubble inclusions. They were light yellow in colour, except the $Ca_9(La,Yb)(VO_4)_7$, which was light green in colour and showed low transparency. The phase analysis showed the absence of impurity phases in the grown crystals. According to the chemical analysis data, the total concentration of trace impurities for each crystal did not exceed $2 - 5\times10^{-3}$ weight %.

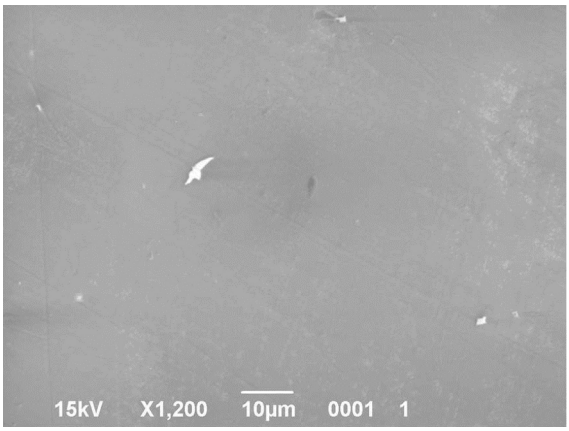

Fig.1. SEM image of the $Ca_9La(VO_4)_7$:Yb crystal surface (compositional contrast mode).

3.1 Chemical compositions

It is known, that the formation of ferroelectric domains and their characteristics depend on the chemical composition of ferroelectric crystals (see, for example [39]). Thus, $Ca_9La(VO_4)_7$ and $Ca_{10}Li(VO_4)_7$ crystals were studied in raster scanning mode on an electron microscope with an X-ray microanalyzer. The concentrations of host elements in the Czochralski grown single crystals are presented in Tables 1-3. In the $Ca_9La(VO_4)_7$ crystal, the concentrations of calcium, lanthanum and vanadium corresponded to the stoichiometric composition within the measurement error (Table 1). For the Yb-doped $Ca_9La(VO_4)_7$ crystal, the concentrations of calcium, R (lanthanum+ytterbium) and vanadium corresponded to the stoichiometric composition within the measurement error (Table 2). An analysis of the sample surface revealed the presence of Yb-enriched regions. Figure 1 shows an image of the $Ca_9La(VO_4)_7$:Yb crystal in the reflection geometry (the composition contrast mode). Bright areas correspond to regions with larger Z_{eff} values. The typical sizes of the Yb-enriched regions are up to 10 μm (Figure 1). Thus, low transparency of the $Ca_9La(VO_4)_7$:Yb single crystal is due to the formation of amorphous inclusions enriched by Yb.

For the $Ca_{10}Li(VO_4)_7$ crystal, concentrations of calcium and vanadium correspond the stoichiometric composition (Table 3). The Li content was not determined due to experimental limitations of the X-ray microanalyzer for light elements.

Table 1. Concentration of host elements in the $Ca_9La(VO_4)_7$ crystal

	C_{La}, wt.%	C_{Ca}, wt.%	C_V, wt.%
Nominal	10.65	27.66	26.11
Crystal	10.66±0.53	27.66±1.38	27.34±1.37

Table 2. Concentration of host elements in the $Ca_9La(VO_4)_7$:Yb crystal

	C_{La}, wt.%	C_{Yb}, wt.%	C_{Ca}, wt.%	C_V, wt.%
Nominal	9.00	1.99	27.55	27.23
Crystal	9.43±0.47	1.45±0.07	27.54±1.38	27.32±1.37
Inclusion	3.58±0.18	50.62±2.53	12.55±0.63	11.54±0.58

Table 3. Concentration of host elements in the $Ca_{10}Li(VO_4)_7$ crystal

	C_{Li}, wt.%	C_{Ca}, wt.%	C_V, wt.%
Nominal	0.57	33.06	29.41
Crystal	-	33.12±1.66	30.06±1.50

3.2 Refinement of the crystal structure

Refinement of the structure of $Ca_9La(VO_4)_7$ and $Ca_{10}Li(VO_4)_7$ crystals (data for the latter are given in [15]) shows that both crystals belong to the space group *R*3*c* (Table 4). Information on the crystal structure defects of the grown crystals was obtained by analyzing rocking curves for different reflections and is presented in Table 5.

Analysis of high-resolution diffraction results including the rocking curves and diffuse scattering, show that the dispersion of the lattice parameters (nodes elongation in q_z axis) over the entire irradiated area (several mm^2) is negligible.

A detailed study of the defect structure of the grown $Ca_{10}Li(VO_4)_7$ single crystal was described [15]. This crystal was shown to have a block structure. Two blocks were found whose boundaries were parallel to the sample surface and offset by approximately 4 arc minutes. Moreover, a slight asymmetry was observed in the diffuse scattering of q_z values in the reciprocal lattice maps. It indicates the presence of point defects, probably vacancies [15].

3.3 Ferroelectric-domain structure

A domain strip-like structure characterized by a period of ~10 μm was observed in the $Ca_9La(VO_4)_7$ crystal (Figure 2). Adjacent domains were identical, as observed in linearly polarized light. This effect is possible if spontaneous electric polarizations in neighboring domains are directed opposite to each other and parallel to the third-order axis. In this case, the optical indicatrices in neighboring domains are ellipsoids of rotation around the third-order axis of the crystal. The cross sections of ellipsoids by a plane perpendicular to the third-order axis will be a circle. This makes it impossible to distinguish adjacent domains in linearly polarized light. Typically, such domains can be distinguished by applying an electric field to the crystal. In this case, the ferroelectric domain structure can be visualized due to the scattering and reflection of light from 180° domain walls in the absence of an external electric field. The high Curie temperature of binary whitlockite-related phosphate and vanadate crystals is an indicator that the domain structure is actually insensitive to applied external electric fields and mechanical stress at room temperatures. The $Ca_9La(VO_4)_7$:Yb crystal was not studied by the polarization-optical method due to its low optical transparency.

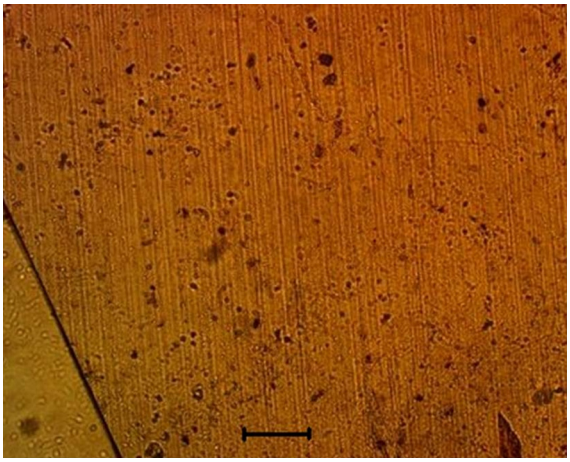

Fig. 2. Ferroelectric domains with a period of ~ 10 μm in the $Ca_9La(VO_4)_7$ single crystal. The photograph was taken in linearly polarized white light passing along the third-order axis. The marker corresponds to a distance of 100 μm

Optical activity and spontaneous birefringence of light were not observed in the

Table 4. Refined lattice parameters, a, c, axial ratio, c/a, and cell volume, V, for studied $Ca_9La(VO_4)_7$, $Ca_9La_{1-x}Yb_x(VO_4)_7$, $Ca_9Yb(VO_4)_7$ crystals. The Yb molar content obtained assuming the Vegard's rule and the side data of (b) and (c) for $Ca_9La_{1-x}Yb_x(VO_4)_7$ is 11.8% Yb.

Crystal	$Ca_3(VO_4)_2$	$Ca_9La(VO_4)_7$	$Ca_9La(VO_4)_7$	$Ca_9La_{1-x}Yb_x(VO_4)_7$	$Ca_9Yb(VO_4)_7$
Method of sample production	SC	PC	CZ	CZ	PC
XRD method	LSCXRD	LPXRD	SPXRD	HRLPXRD	LPXRD
a, Å	10.809(1)	10.8987(5)	10.89554(1)	10.89295(2)	10.8564(5)
c, Å	38.028(9)	38.147(1)	38.14099(3)	38.12619(7)	37.924(1)
c/*a*	3.5182(1)	3.5047(1)	3.500606(1)	3.500080(1)	3.49324(2)
V, Å^3	3847.7(9)	3924.1(3)	3921.208(7)	3917.82(2)	3870.9(3)
T, K	RT	297	298(3)	297(3)	RT
Reference	[40]	[1]	This work	This work	[4]

SC – single crystal, PC – polycrystals synthesized by solid state reaction, CZ – Czochralski grown crystal; LSCXRD – laboratory single-crystal diffraction, LPXRD – laboratory X-ray powder diffraction, SPXRD – X-ray powder diffraction using a high-resolution instrument and synchrotron beam, HRLPXRD – laboratory X-ray powder diffraction using an instrument equipped with a monochromator and strip detector.

$Ca_{10}Li(VO_4)_7$ crystal. A strip-like domain structure was also not detected. It should be noted that the $Ca_{10}Li(VO_4)_7$ crystal is more sensitive to annealing conditions and mechanical treatment compared to the $Ca_9La(VO_4)_7$ crystal. These factors cause the appearance of optical birefringence. Therefore, we suggest that the antiferroelectric phase with a center of symmetry is formed in the $Ca_{10}Li(VO_4)_7$ crystal as a result of a high temperature phase transition. This effect has been observed for other whitlockite-related crystals [41, 42]. Stabilizing spontaneous polarization and accompanying spontaneous deformation were not detected in the antiferroelectric crystal. This may result in high sensitivity to mechanical stress. Induced mechanical stresses can cause decompensation of antiferroelectric sublattices, the occurrence of spontaneous polarization and optical birefringence.

3.4 Mechanical properties

Comparison of mechanical characteristics of the $Ca_9La(VO_4)_7$ and $Ca_{10}Li(VO_4)_7$ single crystals confirms the above-mentioned suggestion. As it is seen from Table 5, the maximum hardness H_v was observed for the $Ca_9La(VO_4)_7$ single crystal, the minimum value – for the $Ca_{10}Li(VO_4)_7$ crystal. The difference is about 27%. The ytterbium doping causes a decrease in the hardness H_v by ~16% and leads to an increase in K_{1c} by ~20%.

Generally, the Vickers hardness H_v of the $Ca_9La(VO_4)_7$ crystal is close to the Vickers hardness H_v of the crystals of the isostructural solid solution $Ca_9Y(VO_4)_{7-x}(PO_4)_x$ measured for the same crystallographic plane under the same load [27].

The ratio K_{1c}/H_v can be used as a parameter defining the transition "from brittle to ductile state". [43]. For the $Ca_9La(VO_4)_7$ crystal doped with Yb, shifts to the "ductile" side compared to the pure crystal. For the $Ca_{10}Li(VO_4)_7$ crystal, the value K_{1c}/H_v, is close to that of the $Ca_9La(VO_4)_7$ crystal.

4. Conclusions

The observed diversity of properties of binary orthovanadates belonging to the whitlockite family is associated, in particular, with differences in the distribution of cations over the 5 crystallographic cation sites. This distribution depends on ionic radii of cations, while the existence of vacancies in crystal lattices of these compounds depends on the charge of the calcium substituting cation. The influence of the calcium substitution mechanism during the formation of binary orthovanadates on peculiarities of crystal structure, domain formation, and mechanical characteristics of $Ca_9La(VO_4)_7$ and $Ca_{10}Li(VO_4)_7$ single crystals grown by the Czochralski method is shown. The high-resolution diffraction method made it possible to obtain high-quality powder diffraction data as well as information on the structure and perfection of crystals. Refinement of the structure using the Rietveld approach allowed us to determine the lattice parameters and site occupancy. Calcium substitution mechanisms have a significant impact on domain formation in binary vanadate crystals. Based on polarization-optical studies, the formation of a ferroelectric domain strip-like structure with a spontaneous polarization direction parallel to the three-order axis was

Table 5. Lattice parameters and crystal imperfection characteristics obtained from high-resolution diffraction data

		$Ca_9La(VO_4)_7$	$Ca_{10}Li(VO_4)_7$ (*)
Unit cell parameters	*a*, Å	10.8959(2)	10.81450(7)
	c, Å	38.1416(7)	38.0657(3)
	V, Å^3	3921.5(2)	3855.47(8)
	ρ, g/cm^3	3.254	3.133
FWHM of rocking curve		0.019°(reflection 0 0 30)	0.025° (reflection 0 0 30), 0.044° (reflection 1 0 16)
Comments		Single block	Two blocks, their borders parallel to the sample surface, misorientation about 4 arc min*

(*) – the data in this column are from ref. [15].

Table 6. Vickers hardness H_v and the fracture toughness K_{1c} of $Ca_9La(VO_4)_7$ and $Ca_{10}Li(VO_4)_7$ crystals for the (001) plane.

	$Ca_9La(VO_4)_7$	$Ca_9La(VO_4)_7$:Yb	$Ca_{10}Li(VO_4)_7$
H_v, GPa	4.06±0.2	3.41±0.17	2.95±0.15
K_{1c}, MPa·m$^{0.5}$	0.44±0.02	0.53±0.03	0.34±0.02
K_{1c}/H_v, ×10^3 m$^{0.5}$	0.108	0.155	0.115

established in the $Ca_9La(VO_4)_7$ single crystal. $Ca_{10}Li(VO_4)_7$ is found to be antiferroelectric at room temperature.

The Vickers hardness H_v of $Ca_{10}Li(VO_4)_7$ crystals is 27% lower than the hardness of $Ca_9La(VO_4)_7$ crystals. The ratios K_{1c}/H_v characterizing the "brittle-to-ductile" transition are close in $Ca_{10}Li(VO_4)_7$ and $Ca_9La(VO_4)_7$ crystals.

Acknowledgments

A part of this work was supported through the Agreement between Polish Academy of Sciences and National Academy of Sciences of Ukraine. Moreover, investigations are supported by funding through the EURIZON project #3006, which is funded by the European Union under grant agreement No.871072.

We acknowledge the European Synchrotron Radiation Facility (ESRF) for provision of synchrotron radiation facilities and we would like to thank NAME for assistance and support in using beamline ID22. The work presented in this paper benefits from the support received from the Polish Ministry of Science and Higher Education, dec. no. 2021/WK/11.

References

1. A.A. Belik, V.A. Morozov, S.S. Khasanov, B.I. Lazoryak, *Crystallography Reports*, **42(5)**, 751 (1997).
2. A.A. Belik, V.A. Morozov., R.N. Kotov, S.S. Khasanov, B.I. Lazoryak, *Crystallography Reports*, **45(3)**, 389 (2000).
3. A.A. Belik, V.A. Morozov, S.V. Grechkin, S.S. Khasanov, B.I. Lazoryak, *Crystallography Reports*, **45(5)**, 728 (2000).
4. A.A. Belik, S.V. Grechkin, L.O. Dmitrienko, V.A. Morozov, S.S. Khasanov, B.I. Lazoryak, *Crystallography Reports*, **45(6)**, 976 (2000).
5. W. Paszkowicz, A. Shekhovtsov, M. Kosmyna, P. Loiko, E. Vilejshikova, R. Minikayev, P. Romanowski, W. Wierzchowski, K. Wieteska, C. Paulmann, E. Bryleva, K. Belikov, A. Fitch, *Nuclear Instruments and Methods in Physics Research B*, **411**, 100 (2017).
6. H.K. Kim, M.S. Kim, S.M. Park, A.W. Sleight, *J. Crystal Growth*, **219(1-2)** 61 (2000).
7. Z. Lin, G. Wang, L. Zhang, *J. Crystal Growth*, **304(1),** 233 (2007).
8. Z. Chen, D. Wang, L. Liu, F. Yuan, Y. Huang, L. Zhang, Z. Lin, *J. Alloys and Compounds*, **938**, 168651 (2023).
9. J.S.O. Evans, J. Huang, A.W. Sleight, *J. Solid State Chemistry*, **157(2)**, 255 (2001).
10. X. Hu, X. Chen, N. Zhuang, R. Wang, J. Chen, *J. Crystal Growth*, **310**, 5423 (2008).
11. L. Li, G. Wang, Y. Huang, L. Zhang, Z. Lin, G. Wang, *J. Crystal Growth*, **314**, 331 (2011).
12. D. Petrova, D. Deyneko, S. Stefanovich, S. Aksenov, B. Lazoryak, *Powder Diffraction*, **32(3)**, 175 (2017).
13. S. Liu, C. Li, J. Jiao, Y. She, T. Zhang, D. Ju, N. Ye, Z. Hu, Y. Wu, *Inorganic Chemistry Frontiers*, **11(8)**, 2384 (2024).

14. M.B. Kosmyna, B.P. Nazarenko, I.O. Radchenko, A.N. Shekhovtsov, *Functional Materials*, **22(4)**, 446 (2015).
15. M.B. Kosmyna, B.P. Nazarenko, V.M. Puzikov, A.N. Shekhovtsov, W. Paszkowicz, A. Behrooz, P. Romanowski, A.S. Yasukevich, N.V. Kuleshov, M.P. Demesh, W. Wierzchowski, K. Wieteska, C. Paulmann, *J. Crystal Growth*, **445**, 101 (2016).
16. R. Singh, S.J. Dhoble, *J. Luminescence*, **28(4)**, 607 (2013).
17. L. Li, X.G. Liu, H.M. Noh, J.H. Jeong, *J. Solid State Chemistry*, **221**, 95 (2015).
18. J. Zhao, C. Guo, J. Yu, R. Yu, *Optics & Laser Technology*, **45**, 62 (2013).
19. M.V. Dobrotvorskaya, Yu.N. Gorobets, M.B. Kosmyna, P.V. Mateichenko, B.P. Nazarenko, V.M. Puzikov, A.N. Shekhovtsov, *Crystallography Reports*, **57(7)**, 959 (2012).
20. M.B. Kosmyna, B.P. Nazarenko, V.M. Puzikov, A.N. Shekhovtsov, *Acta Physica Polonica A*, **123(2)**, 305 (2013).
21. L. Liu, R.J. Xie, N. Hirosaki, Y. Li, T. Takeda, C.N. Zhang, et al, *J. American Ceramic Society*, **93(12)**, 4081 (2010).
22. C. Zhang, C. Yao, *Ceramics International*, **49(8)**, 13000 (2023).
23. M.P. Demesh, A.S. Yasukevich, A.N. Shekhovtsov, M.B. Kosmyna, W. Paszkowicz, N.V. Kuleshov, *J. Luminescence*, **224**, 117270 (2020).
24. B.I. Lazoryak, A.A. Belik, S.Y. Stefanovich, V.A. Morozov, A.P. Malakho, O.V. Baryshnikova, I.A. Leonidov, O.N. Leonidova, *Doklady Physical Chemistry*, **384**, 144 (2002).
25. V.A. Morozov, A.A. Belik, S.Y. Stefanovich, V.V. Grebenev, O.I. Lebedev, G. Van Tendeloo, B.I. Lazoryak, *J. Solid State Chemistry*, **165(2)**, 278 (2002).
26. B.I. Lazoryak, V.A. Morozov, A.A. Belik, S.Y. Stefanovich, V.V. Grebenev, I.A. Leonidov, E.B. Mitberg, S.A. Davydov, O.I. Lebedev, G. Van Tendeloo, *Solid state sciences*, **6(2)**, 185 (2004).
27. M.B. Kosmyna, P.V. Mateychenko, B.P. Nazarenko, A.N. Shekhovtsov, S.M. Aksenov, D.A. Spassky, A.V. Mosunov, S.Yu. Stefanovich, *J. Alloys and Compounds*, **708**, 285 (2017).
28. B. Lazoryak, D. Deyneko, S. Aksenov, V. Grebenev, S. Stefanovich, K. Belikov, M. Kosmyna, A. Shekhovtsov, A. Sulich, W. Paszkowicz, *CrystEngComm*, **20**, 6310 (2018).
29. Z. Zhang, P. Loiko, H. Wu, X. Mateos, J.M. Serres, H.F. Lin, W.D. Chen, G. Zhang, L.Z. Zhang, F. Díaz, M. Aguiló, V. Petrov, U. Griebner, Y.C. Wang, E. Vilejshikova, K. Yumashev, Z.B. Lin, *Optical Materials Express*, **7(2)**, 484 (2017).
30. G. Liu, Z. Bai, F. Yuan, Y. Huang, L. Zhang, Z. Lin, *J. Crystal Growth*, **520**, 62 (2019).
31. A. Pajączkowska, *Acta Physica Polonica A*, **124(2)**, 171 (2013).
32. W. Paszkowicz, *Nuclear Instruments and Methods in Physics Research A*, **551(1)**, 162 (2005).
33. A. Zięba, W. Dabrowski, A. Czermak, *Proceedings of the First Polish Meeting High-Resolution X-ray Diffractometry and Topography of Conferences Notes*, Szklarska Poremba, 14-17 September, 63 (1996) (In Polish).
34. H. Toraya, H. Hibino, K. Ohsumi, *J. Synchrotron Radiation*, **3(2)**, 75 (1996).
35. J.L. Hodeau, P. Bordet, M. Anne, A. Prat, A.N. Fitch, E. Dooryhee, G. Vaughan, A.K. Freund, *Proceedings of SPIE's International Symposium on Optical Science, Engineering, and Instrumentation*, **3448**, 353 (1998).
36. A. Fitch, *J. Research of National Institute of Standards and Technology*, **109**, 133 (2004).
37. J. Rodríguez-Carvajal, *Physica B*, **192**, 55 (1993).
38. A.G. Evans, E.A.Charles, *J. American Ceramic Society*, **59(7-8)**, 371 (1976).
39. N.F. Evlanova, I.I. Naumova, T.O. Chaplina, S.V. Lavrishchev, S.A. Blokhin, *Physics of the Solid State*, **42**, 1727 (2000).
40. R. Gopal, C. Calvo, *Zeitschrift fuer Kristallographie, Kristallgeometrie, Kristallphysik, Kristallchemie*, 137, 67 (1973).
41. A.V. Teterskii, S.Y. Stefanovich, B.I. Lazoryak, D.A. Rusakov, *Russian J. Inorganic Chemistry*, **52**, 308 (2007).
42. S.Yu. Stefanovich, A.A. Belik, M. Azuma, M. Takano, O.V. Baryshnikova, V.A. Morozov, B.I. Lazoryak, O.I. Lebedev, G. Van Tendeloo, *Physical Review B*, **70**, 172103 (2004).
43. G. Fantozzi, G. Orange, K. Liang, .M. Gautier, J-P Duraud, P Maire, C Le Gressus, E. Gille, *J. American Ceramic Society*, **72(8)**, 1562 (1989).